Progress of Theoretical Physics, Vol. 69, No. 5, May 1983

Transition from Torus to Chaos Accompanied by Frequency Lockings with Symmetry Breaking

—— *In Connection with the Coupled-Logistic Map* ——

Kunihiko KANEKO

Department of Physics, University of Tokyo, Tokyo 113

(Received December 18, 1982)

Transition from torus to chaos is studied using the coupled-logistic map. We observe the period-adding sequence, which obeys the critical phenomena of a one-dimensional mapping. The fixed Lyapunov exponent is also obtained. The locking that appears after the sequence breaks the symmetry of the system. Self-similar stripe structure of basins is also found. Various properties and a phase diagram of the map are given. The mechanism of the distortion of torus and transition to chaos is also discussed.

§ 1. Introduction

Transition from torus to chaos with or without frequency locking is a fascinating and interesting problem in the field of nonlinear physics.[1)~7)] In previous papers,[8),9)] we studied the regularity of the frequency locking using a one-dimensional mapping. We investigated the "period-adding" sequence and found various scaling properties and explained them by the theory of intermittency and the ansatz of a fixed point function. Shenker studied the Fibonacci sequence for this one-dimensional mapping.[5)]

When we take the Poincarè section of a torus, there remain still two variables, i. e., amplitude and phase. In the previous study of the one-dimensional mappings, we restricted our interest only to the phase variable. It will be of importance, however, to study two-dimensional mappings. We study dissipative systems in this paper and use a map with a non-constant Jacobian. Particularly, we take a coupled-logistic map, that is,

$$\begin{cases} x_{n+1}=1-Ax_n^2+D(y_n-x_n), \\ y_{n+1}=1-Ay_n^2+D(x_n-y_n). \end{cases} \tag{1·1}$$

Using the well-known transformation $A=\lambda(\lambda/4-1/2)$, $x'=(x-1/2)/(\lambda/4-1/2)$, and $y'=(y-1/2)/(\lambda/4-1/2)$, we can write $x'_{n+1}=\lambda x_n'(1-x_n')+D(y_n'-x_n')$ and $y'_{n+1}=\lambda y'_n(1-y_n')+D(x_n'-y_n')$. Thus this map represents a system with two logistic models coupled by a linear term. It can be regarded as a simple model of two coupled systems,[10)~12)] each of which exhibits a period-doubling bifurcation route to chaos. This map may serve us to understand how coupled oscillators, such as Josephson junction or chemically reacting cells, show various

behaviors, for example, entrainment, quasi-periodicity and chaos.

The map (1·1) is simple among maps with non-constant Jacobian, which have been less studied than the case of a constant Jacobian. It exhibits, however, various phases, such as cycles, torus, frequency locking, chaos and hyperchaos, as will be shown later. In this paper we focus our attention mainly on the mechanism of the frequency locking at the transition from torus to chaos.

In § 2, a phase diagram and some general results for the map (1·1) are given. Various types of the attractors (torus, chaos and hyperchaos[13]) are classified by the Lyapunov exponents.

In § 3, the period-adding sequence of the frequency locking is studied according to the theory of a one-dimensional mapping.[8),9)] Various scalings and the similarity of the Lyapunov exponents will be checked.

In § 4, we discuss the frequency locking accompanied by the symmetry breaking, which was found for the map (1·1). After this symmetry breaking occurs, the oscillations of the two cells (that is, x and y) become different and two types of the oscillations appear. The basin of each oscillation is also studied. It is very complicated and it will be difficult to tell which type of oscillations appears from a given initial value. Especially, two basins form a stripe structure in a self-similar manner near the line $y=x$.

The transition from torus to chaos has been observed in various two-dimensional mappings. If we restrict ourselves to the local properties of the frequency locking, the previous theory of scalings in a one-dimensional mapping[9)] is valid. However, global properties must be studied in order to understand the transition to chaos and how the dimension of the attractor grows. We discuss this problem in § 5, but detailed study of the global properties are left to future.

This work is essentially based on the unpublished note, which was completed earlier than the one-dimensional theory.[8),9)]

§ 2. Phase diagram and general aspects of the coupled-logistic map

In this section, we give some analytic properties and the phase diagram of the

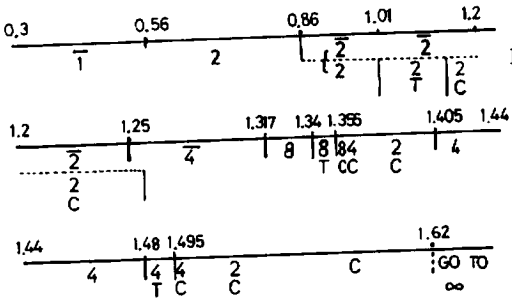

Fig. 1. The rough phase diagram of the coupled-logistic map (1·1) with $D=0.1$. The n-cycle with $x=y$ is denoted by $\bar{n}$; while the one with $x\neq y$ is denoted by n. The m-torus and n-chaos (see the text for these terminologies) are represented by mT and nC, respectively. For $0.86\leq A\leq 1.26$, the attractors are splitted into two basins, which are written in two lines.

map (1·1). Especially, the case $D=0.1$ is studied in detail. For the case $D=0$, the map (1·1) is decomposed into two independent logistic maps, which show the period-doubling bifurcations to chaos[14] ($1\to2$ at $A^{(2)}=0.75$, $2\to4$ at $A^{(4)}=1.25$, $4\to8$ at $A^{(8)}\simeq1.368$, $\cdots$, and $A^{(\infty)}\simeq1.401155\cdots$). If a uniform state ($x=y$) is stable, the phase diagram is the same as $D=0$. The condition for the stability of a uniform state is given as follows.

Using the transformation $\xi_n=(x_n+y_n)/2$ and $\eta_n=(x_n-y_n)/2$, we have,

$$\begin{cases}\xi_{n+1}=1-A(\xi_n^2+\eta_n^2),\\ \eta_{n+1}=-2\eta_n(A\xi_n+D).\end{cases} \tag{2·1}$$

Thus, η_n is given by

$$\eta_n=\prod_{k=0}^{n-1}(-2(A\xi_k+D))\eta_0\,. \tag{2·2}$$

The stability of the state $x_k=y_k=\xi_k$(i.e., $\eta=0$) is given by

$$\left|\prod_{k=1}^{p}(-2(Ax_k+D))\right|<1\,, \tag{2·3}$$

where p is the period for the logistic map and it takes infinity for chaotic states. For example, the fixed point $(x=y=(\sqrt{1+4A}-1)/(2A)$ for $A<3/4)$ is stable for $|2D-1+\sqrt{1+4A}|<1$ and the two-cycle $(x_{1,2}=y_{1,2}=(1\pm\sqrt{4A-3})/(2A)$ for $A<5/4)$ is stable for $|1+D+D^2-A|<1/4$. Perturbation theory for uniform states are given in Ref. 10).

We note that from Eq. (2·2)

$$\prod_{k=1}^{p}(-2(A\xi_k+D))=1 \tag{2·4}$$

for the general p-cycle point with $x\neq y$.

Afterwards, the results for $D=0.1$ is shown in detail. The rough phase diagram is given in Fig. 1. For $A<0.56$ the fixed point is stable and the two-cycle with $x=y$ is stable for $0.86<A<1.25$ from the stability condition given above. There exists a two-cycle point with $x\neq y$, which is given by

$$\begin{cases}\xi_1=\xi_2=(1/2-D)/A=0.4/A\,,\\ \eta_1=-\eta_2=\{A-[(1-D)^2-1/4]\}^{1/2}=(A-0.56)^{1/2}\end{cases} \tag{2·5}$$

for $0.56<A\lesssim1.010$. At $A\simeq1.010$, this cycle loses its stability via a Hopf bifurcation and a two-torus appears. (In this paper, we use a terminology 'torus', regarding that the map is a projection onto a surface from higher dimensional motions, and use a word 'n-torus' for the torus separated by n times (i. e., n-th iterated map gives a single torus).) As we increase the value of A, the transition from torus to chaos with frequency lockings occurs. We note that the cycle with

$x=y$ (period-two for $A<1.25$ and period-four for $A>1.25$) and the state with $x\neq y$ coexist for $0.86<A\lesssim 1.26$. At $A\simeq 1.26$, the chaos with $x\neq y$ becomes unstable and only the 4-cycle with $x=y$ remains.

The 4-cycle becomes unstable at $A\simeq 1.317$, and an 8-cycle with $x\neq y$ appears,

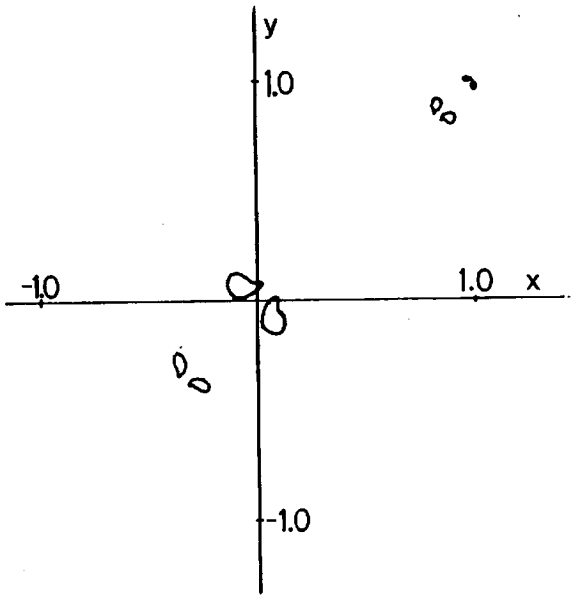

Fig. 2. (a)$A=1.350$ (8T)

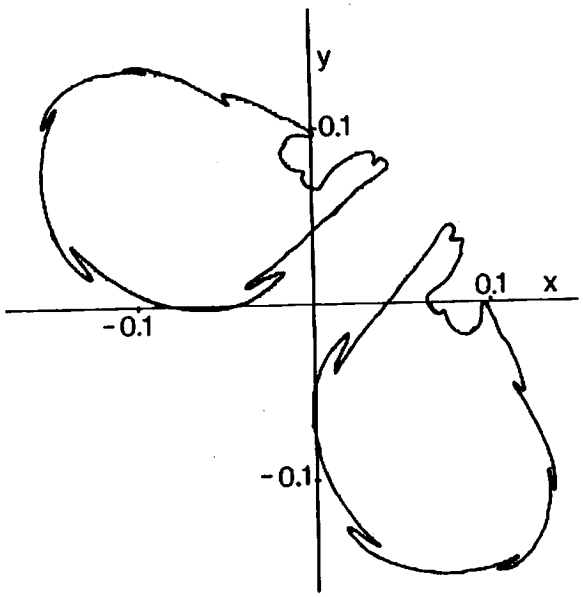

(b)$A=1.3525$ (8T) (only the region $|x|<0.2$ and $|y|<0.2$)

(continued)

which becomes unstable and an 8-torus appears at $A \simeq 1.34$. The torus goes to chaos accompanied by frequency lockings. We study this transition in detail in latter sections. The figures of the attractors are given in Figs. 2(a), (b) (8-torus), (c) (8-chaos), (d) (4-chaos) and (e) (two-chaos). We use a word "n-chaos" for

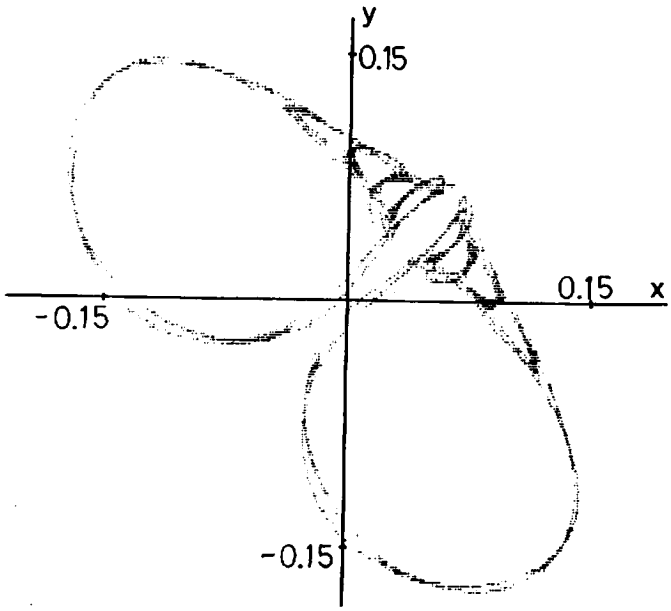

(c) $A=1.355$ (8C) (only the region $|x|<0.2$ and $|y|<0.2$)

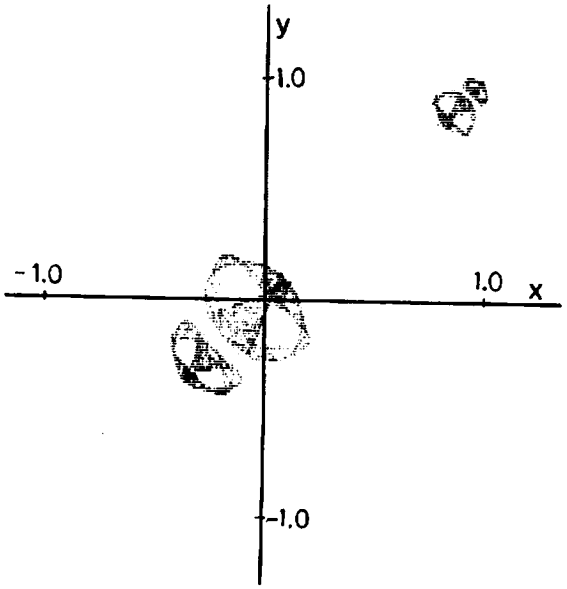

(d) $A=1.373$ (4C)
(continued)

the chaos decomposed into n regions. The fusion of chaos ($8C \to 4C \to 2C$) is analogous to the band merging in a logistic map,[14] but it is not clear, whether the mechanism of this fusion can be explained through a one-dimensional mapping or not. As we increase the value of A further, a 4-cycle appears via intermittency,

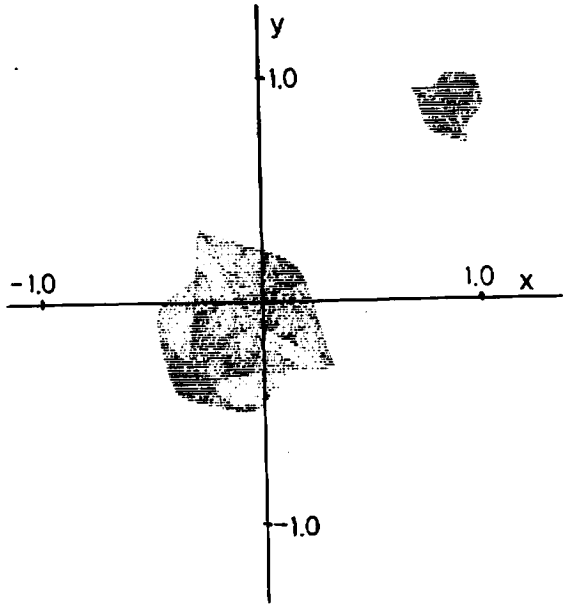

(e) $A=1.40$ (2C)

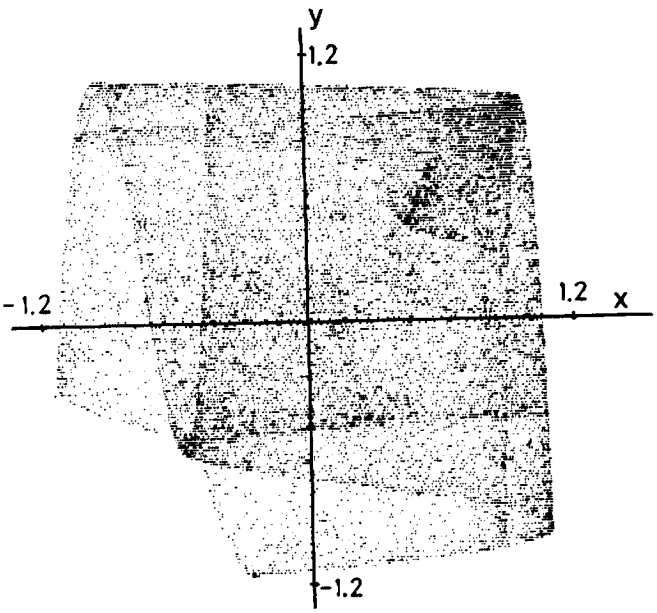

(f) $A=1.55$ (hyperchaos)

Fig. 2. The attractor of the map (1·1) with $D=0.1$ for (a)~(f)

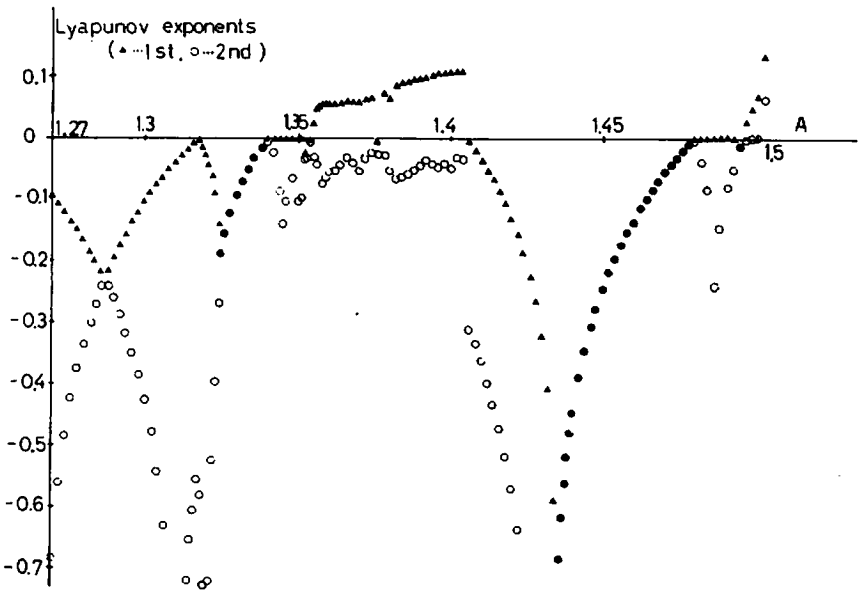

Fig. 3. The first and second Lyapunov exponents. We took 200000 iterations for the calculations.

which loses its stability through a Hopf bifurcation and again the transition from torus to chaos with frequency lockings occurs.

In order to check this phase diagram quantitatively, the Lyapunov exponents are calculated, which are shown in Fig. 3. Two Lyapunov exponents are positive for $A \gtrsim 1.50$ and Rössler's hyperchaos[13] exists (see Fig. 2(f) for the attractor).

Thus, we can see the transition "cycle→(doubling)→longer cycle→(Hopf bifurcation)→torus→various frequency lockings→chaos→evolution of chaos→(fusion of chaos)→hyperchaos" in our model.

§ 3. Scaling of the period-adding sequence at the frequency locking

In this section we study the similarity of the locking states. Here and in what follows, we express the period by the value divided by 8 (i. e., n-cycle means $8n$-cycle for the original map (1·1)), since the 8th-iterated structure as is seen in Fig. 2(a) is always conserved for $A \lesssim 1.3555$, where the transition 8C→4C occurs. The periods of the stable cycles which appear from $A=1.3500$ to 1.3544 are given in Figs. 4(a), (b) and (c).

The sequence of the periods that is easiest to observe in this region is given by

$$Q_n = 8n - 1 \qquad (3\cdot1)$$

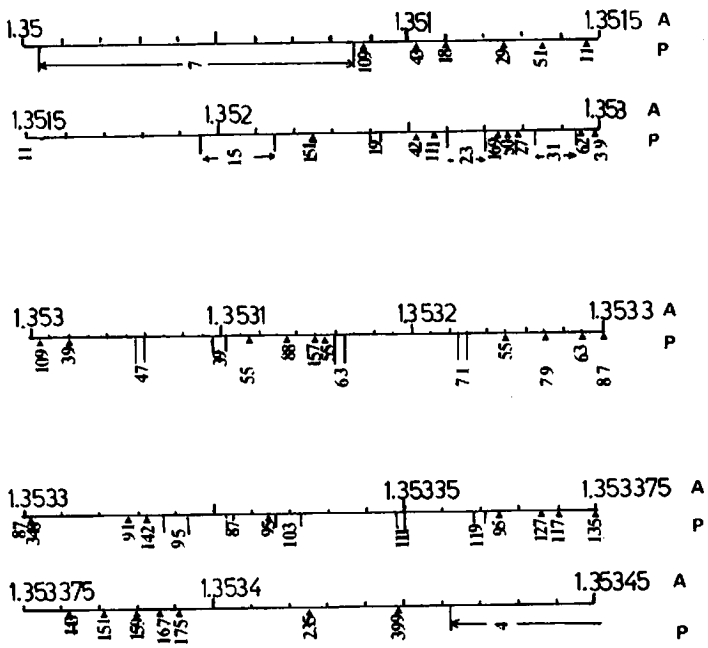

Fig. 4. The periods of stable cycles (lockings) which appear
(a)from $A=1.350$ to 1.353 (we increase the parameter A by 0.000025),
(b)from $A=1.353$ to 1.3533 (we increase the parameter A by 0.000005),
(c)from $A=1.35330$ to 1.35345 (we increase the parameter A by 0.000001).
We regard the attractor as p-cycle if (x_{400000}, y_{400000}) coincides with $(x_{400000+8p}, y_{400000+8p})$ with the accuracy of 10^{-8}. The values of p are written below the line. If no value is written, there is no cycle with the period shorter than 2500.

with the rotation number

$$w_n=P_n/Q_n=2n/(8n-1), \tag{3·2}$$

where P_n is the number of the rotations around the center of a torus during Q_n cycles. We define A_n by the value at which the Q_n-cycle appears. As n goes to infinity, the rotation number converges to $1/4$ and A_n to $A_\infty=1.35343075\cdots$, after which the stable 4-cycle appears. We have plotted $\log(A_\infty-A_n)$ vs $\log n$ in Fig. 5, which shows

$$A_\infty-A_n=0.0148\times n^{-2} \tag{3·3}$$

as n goes large. The width $\Delta A_n\equiv A_n^f-A_n$ (A_n^f is the value of A, where the Q_n-cycle loses its stability) obeys the scaling $\Delta A_n\propto n^{-3}$ (see Fig. 5). We have also studied the distance of nearest periodic points ΔR_n and verified $\Delta R_n\propto n^{-2}$. Thus, the critical exponent is the same as the one-dimensional case.[8),9)]

Next, we study to which category of Ref. 9) this sequence belongs. The local

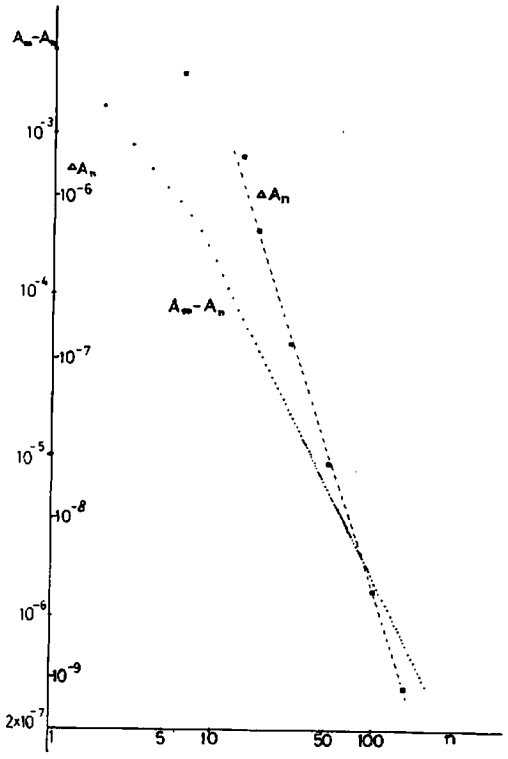

Fig. 5. Scaling properties of the period-adding sequence ($(8n-1)$-sequence). The quantities $(A_\infty - A_n)$ ($\cdot$) and A_n ($\blacksquare$) vs n are plotted.

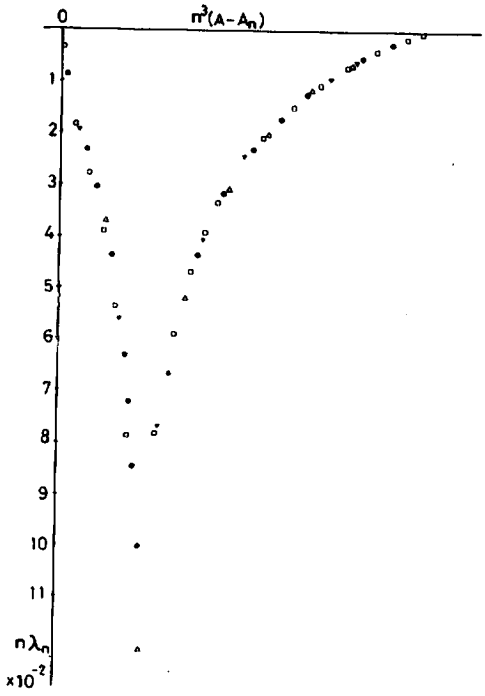

Fig. 6. The similarity of the first Lyapunov exponent λ_n. The Lyapunov exponent is scaled by n^{-1}, while $(A-A_n)$ is scaled by n^{-3}. ●, △, ▼ and □ show the scaled exponents for $n=14$, 18, 30 and 101, respectively.

period-doubling bifurcation occurs for $n \geq 5$ (e. g., $39 \to 78 \to 156 \to 312 \to \cdots \to$ chaos), which obeys the theory of Feigenbaum. Thus, this sequence belongs to the Case III of § 4 of Ref. 9). The scaled first Lyapunov exponent ($n\lambda_n$ as a function of $n^3(A-A_n)$) is given in Fig. 6, which seems to assure the existence of the fixed point function.[9] We note the similarity between Fig. 6 and Fig. 6(c) or Fig. 9 of Ref. 9). The second Lyapunov exponent is large in magnitude compared with the first and the variation of it is small. The application of the theory of the one-dimensional mapping, therefore, seems to be justified.

Thus, the numerical results reproduce the one-dimensional theory based on the tangent bifurcation and the existence of a fixed point function.

§ 4. Frequency locking with symmetry breaking

According to the theory based on the map[8),9)]

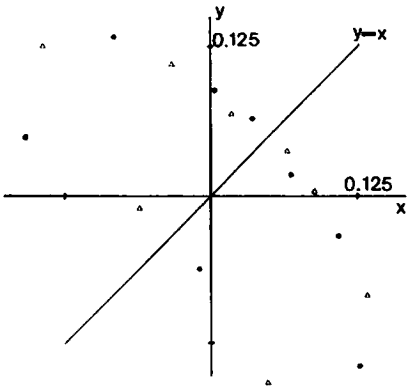

Fig. 7. Two types of the 4-cycles (32-cycle for the original map) at $A=1.35344$. ● and △ denote the two 4-cycles respectively. We have plotted only 8 points nearest to the origin. We note that the cycle △ is a mirror image of the cycle ● about $y=x$.

$$\theta_{n+1}=\theta_n+A\sin(2\pi\theta_n)+D(\mathrm{mod}1), \tag{4·1}$$

there is a sequence with the rotation number $(qn+s)/(pn+r)$ $(n=1, 2, \cdots\cdots)$ between the lockings with q/p and s/r. In this case p and q are relatively prime. The sequence with the rotation number $2n/(8n-1)$ in § 3, however, does not satisfy this property. We also have to note that the period of the locking which appears at A_∞ is not 8 but 4. What is this mechanism?

First, we note that two types of 4-cycles (32-cycle for the original map) coexist. The basin for the attraction breaks into two parts. The attractor is symmetric about $y=x$ for $A<A_\infty$, but each 4-cycle at $A>A_\infty$ is not symmetric about $y=x$ (see Fig. 7). One type of the 4-cycle is a mirror image of the other 4-cycle about $y=x$. Thus, the symmetry

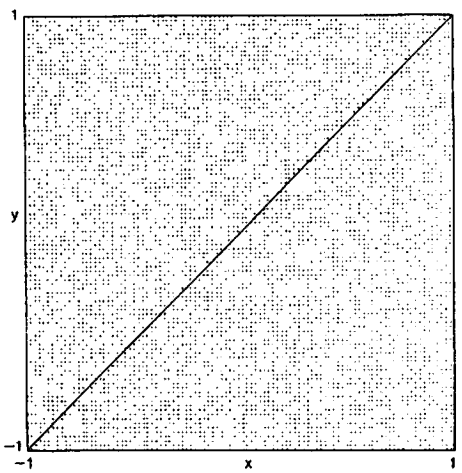

(a) We have studied the map (1·1) with the initial values $(x_0, y_0)=(-1.0+2i/100, -1.0+2j/100)$ $(i, j=1, 2, \cdots, 100)$. If the point $(x_0(i), y_0(j))$ is a basin for the 4-cycle of the type ● of Fig. 4, we have put a dot, while we have not put a dot, if the point is a basin for the 4-cycle of the other type.

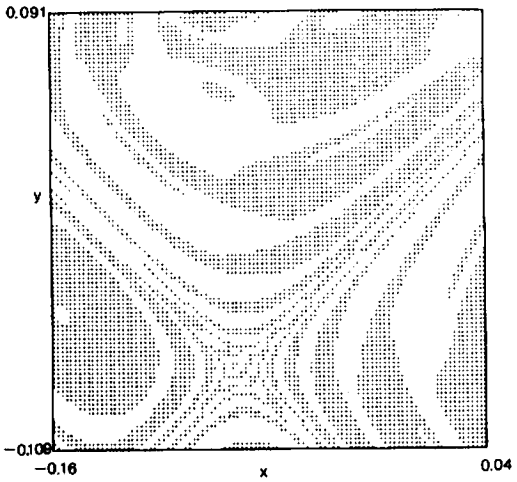

(b) We have increased the resolution of Fig. 8(a). We have studied 100×100 points in $-0.16\le x_0\le0.04$ and $-0.109\le y_0\le0.091$. In this region the 4-cycle of Fig. 7 exists. We note the stripe structure near the line $y=x$.

Fig. 8. The basin for the attraction for each 4-cycle at $A=1.35344$.

breaking occurs at $A=A_\infty$.

For $A<A_\infty$, the cycle (or chaos) consists of two types of the oscillations (i. e., points near one type of the 4-cycle at $A=A_\infty$ and points near the other type) and the transition between the two regimes. The time for the transition grows by $(A_\infty-A)^{-1/2}$ (tangent bifurcation mechanism), which diverges at $A=A_\infty$, and thus the symmetry is broken for $A>A_\infty$. The locking near $A<A_\infty$(e. g., $(8n-1)$-sequence in § 3) is made of the points close to the 4-cycles at $A>A_\infty$ (● and △ in Fig. 7) and of the points between these points. The number of the former points increases as A approaches A_∞ (it increases in proportion to n for the $(8n-1)$-sequence), while the number of the latter does not.

Thus, the period-adding sequence is not $(4n-1)$ but $(8n-1)$. In general, we can conclude that the period-adding sequence with the rotation number $(2qn+s)/(2pn+r)$ appears before the locking q/p, which breaks some symmetry and has two basins.

Next, we study the structure of basins. In Figs. 8(a) and (b), it is shown which type of the 4-cycles appears from a given initial value (x_0, y_0) at $A=1.35344$. The figures are antisymmetric about $y=x$, in the sense that if the point (x_0, y_0) belongs to the basin for one 4-cycle, the point (y_0, x_0) belongs to the basin for the other 4-cycle. This is due to the fact that the map (1·1) is symmetric and the two 4-cycles are mirror images of each other about $y=x$.

First, we note that the structure is very complicated. This will be due to the effect of stretching and folding which appears only in the transient phenomenon for this value of A, and which causes chaos for larger A. Near the line $y=x$ the basins form a self-similar structure (see Fig. 9). Around this value of A, there exists a periodic saddle of period-4 on the line $y=x$ (this is a 4-cycle of the original map (1·1); see § 2). The matrix of the fourth iteration of the map (1·1) linearized around this saddle has an egienvalue $\alpha\approx-1.73(<-1)$. Thus, a zone of a basin at $x<y$ is reduced as $|\alpha|^{-1}$ and appears at $x>y$ (because α is negative). This process is repeated infinitely and makes a self-similar structure of the basin near $y=x$. The value of the scaling factor $|\alpha|^{-1}$ is verified through numerical results (see

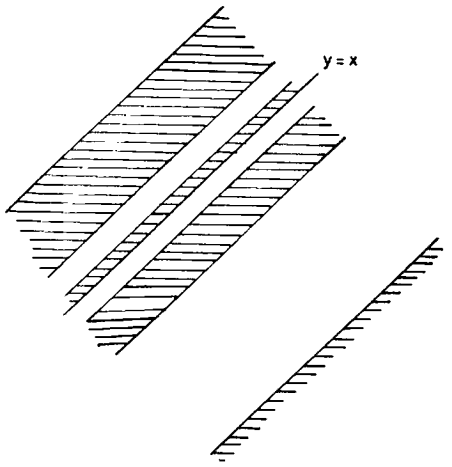

Fig. 9. The stripe structure of the basins around $y=x$. The shaded region is a basin for one 4-cycle, while the blank region is a basin for the other 4-cycle. When we enlarge the figure and increase the resolution by $\alpha^2\simeq3.0$, the same pattern appears.
(The scale of this figure is arbitrary in this sense.)

Fig. 9). We can construct an example of a self-similar structure of basin by using symmetric one-dimensional mappings.[15]

It is interesting to regard that x and y represent the observables of two cells. Then the frequency locking with symmetry breaking of this section can be regarded as the appearance of a spatio-temporal order. At $A>A_\infty$, the oscillations of the two cells become completely different. The formation process of order is treated by many authors for a simple case, that is a relaxation from an unstable point of a double-well potential.[16] The self-similar structure of basins in our problem may give a new aspect of the formation process of order.

It is also important to study the global structure of frequency lockings. For the one-dimensional mapping (4·1) the locking states (devil's staircase)[17] are constructed as follows:

i) $1/2\to1/3\to1/4\to1/5\to\cdots\to1/n\to\cdots\to0/1\,,\quad(n\geq2)$

ii) $1/(n+1)\to2/(2n+1)\to\cdots\to l/(ln+1)\to\cdots\to1/n$

between $1/(n+1)$ and $1/n\,,\qquad(l\geq1)$

iii) $(l+1)/((l+1)n+1)\to(2l+1)/\{(ln+1)+(l+1)n+1\}\to\cdots$
$(ml+1)/\{m(ln+1)+(l+1)n+1\}\cdots\to l/(ln+1)$
between $(l+1)/\{(l+1)n+1\}$ and $l/(ln+1)$, $\qquad(m\geq1)$

⋮

where each sequence is the period-adding sequence (the value q/p is a rotation

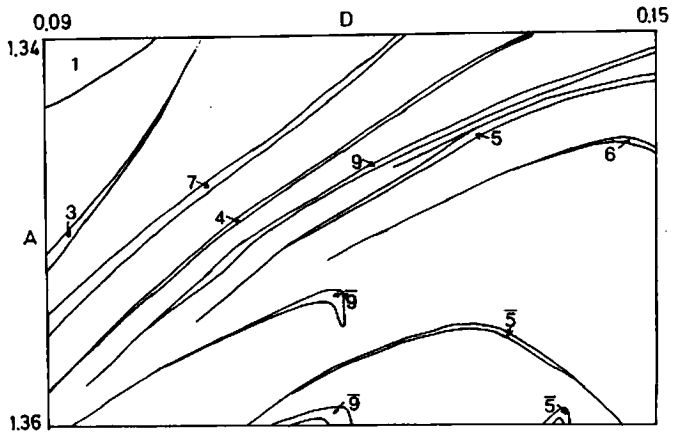

Fig. 10. The frequency lockings around the transition from torus to chaos. The number (1~9) is the period of the stable cycle. We have plotted only cycles with the period shorter than 10. The n-cycle ($8n$-cycle for the original map) which appears after the fusion 8C→4C is represented by $\bar{n}$, which is better to be regarded as $4\times2n$ cycle.

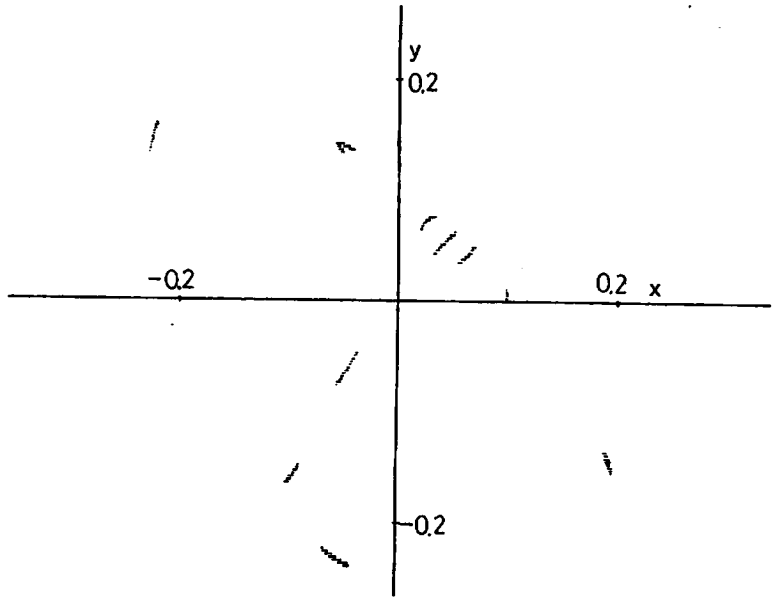

(a)

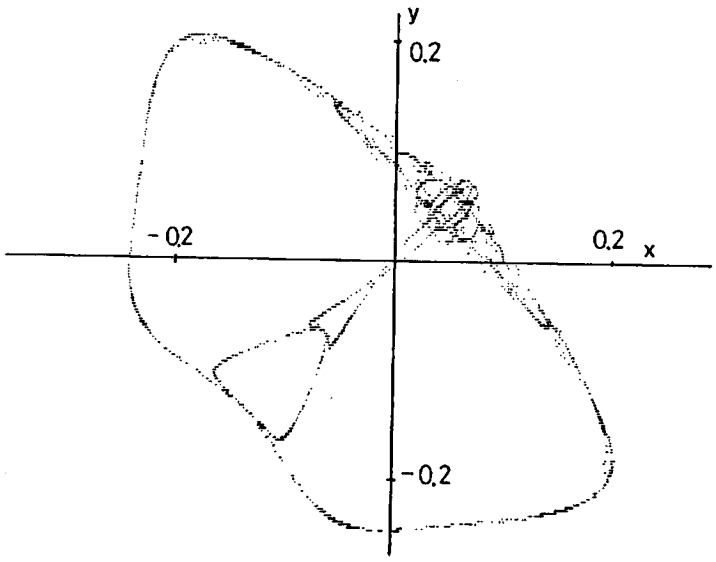

(b)

Fig. 11. The attractor of the map (1·1) with $D=0.14$ for
(a) $A=1.35704$, (only one of the two types of the attractors)
(b) $A=1.35710$.
The chaos is of the type "4C" in our notation and only the region nearest to the origin is shown in these figures.

number and p is a period). We can study in this way the steps of devil's staircase and its similarity, for a one-dimensional mapping.

In our problem, the global structure of lockings is more complex, since there are two types of lockings, i. e., with or without symmetry. The rough phase diagram of frequency lockings is given in Fig. 10, where the number "n" denotes a locking of n-cycle ($8n$-cycle for the original map).

First, we note that there is a period-adding sequence $3\to4\to5\to6\to(\to7\to\cdots)$. These cycles break the symmetry, that is, the attractor is not symmetric about $y=x$ and there exist two types of cycles as is the case for the period 4. There appear lockings with the period 7 (between 3 and 4), 9 (between 4 and 5), 11(between 5 and 6), etc, which is symmetric about $y=x$. The $(8n-1)$-sequence, studied in previous sections, appears between the periods 7 and 4. The lockings of longer periods are constructed in a way similar to the one-dimensional mapping (i), ii), iii), $\cdots$). As is seen in Fig. 10, the locking with symmetry breaking (e. g., 3 or 4 or 5 $\cdots$) occurs at various values of A and D.

For $D\gtrsim1.355$, the transition $8C\to4C$ has already occured, and the cycle for these parameters ($\bar{5}$ or $\bar{9}$ in Fig. 10) has not 8 but 4-iterated structure (i. e., 10×4 or 18×4). The symmetry of the attractor is also broken for the 5-cycles and thus the window with symmetry breaking also occurs for the chaos which has undergone the fusion.

The window ($\bar{5}$ in Fig 10) goes to chaos by the period-doubling bifurcation, as the parameter A is increased. The attractor of this chaos is not symmetric about $y=x$ (see Fig. 11(a)). As the parameter A is increased further, the strange attractor with symmetry appears again (see Fig. 11(b)). Thus, the chaos-chaos transition with symmetry breaking is also observed in our system.

§ 5. Discussion

Transition from tours to chaos accompanied by frequency lockings have frequently been observed in dissipative two-dimensional mappings. The scenario is as follows:

i) Torus appears via a Hopf bifurcation.
ii) The shape of torus is distorted (see Fig. 2(b)).
iii) As the process ii) goes on, the regions of frequency lockings increase. They form a structure of devil's staircase.
iv) Chaos appears through a period-doubling or a tangent bifurcation of some frequency-locked cycle at some value of the bifurcation parameter.
v) The dimension of the attractor[18] increases, which is seen in the increase of two Lyapunov exponents.
vi) As we increase the bifurcation parameter, the sum of two Lyapunov exponents become positive and the attractor covers a two-dimensional

area (see Fig. 2(e)).

vii) Two Lyapunov exponents take positive values (hyperchaos).

This process [i)→vii); it may stop at some step and the inverse process or transition from chaos to cycle through other mechanisms[19)~21)] can occur] was observed in our map (1·1) in various parameter regions and was also observed for other two-dimensional mappings, such as

$$\begin{cases} r_{n+1}=\gamma r_n - g r_n^3 + \tilde{A} r_n \sin(2\pi\theta_n), \\ \theta_{n+1}=\theta_n + \alpha r_n^2 . \qquad (\mathrm{mod}\ 1) \end{cases} \tag{5·1}$$

The distortion of torus ii) was always seen in these examples. It will be related to the oscillation of unstable manifolds of periodic saddles,[22)] which is analogous to the heteroclinic oscillation, well-known in conservative systems.

At the frequency lockings iii), it is easy to observe the period-adding sequence. The scaling properties given in previous papers[8),9)] hold in these examples. Thus, the critical phenomenon of the period-adding sequence seems to be rather universal in two-dimensional mappings.

Though the local mechanism of the onset of chaos can be understood through Feigenbaum's theory[20)] or Pomeau and Manneville's one,[21)] we have to consider global properties, in order to understand the whole process i)→vii). This problem is left to future.

Our mapping (1·1) has a symmetry under the exchange of variables $x \leftrightarrow y$. It is reflected in the properties of the attractor.[23)] The attractors shown in Fig. 1 (such as m, mT, C, mC : ($m=2, 4, 8$)) are symmetric about $y=x$. The attractor with broken symmetry we observed in our map is a cycle, which appears as a frequency locking or chaos, which appears through the doubling of the locking. The critical phenomenon near this locking is ruled by a tangent bifurcation.[8),21)] In this case, however, the period of the period-adding sequence with similarity is not ($pn+q$) but ($2pn+q$) (p is a period of the cycle which appears at $n\to\infty$). The symmery breaking of this type has not yet been studied well. It may give a new insight upon the onset of a spatio-temporal order.

The basin of each cycle with broken symmetry is very complicated, as was shown in Figs. 8(a) and (b). Thus, it will be rather difficult to predict the final state form a given initial value. The complicated structure is typically seen near the sadlle line ($y=x$) as a self-similar stripe structure. This structure is expected to appear near unstable cycles, if one stripe structure of a basin exists. Thus, this structure of a basin may be observed in various nonlinear systems. It is also interesting to study the effect of this structure on the transient phenomena, especially concerning the effect of a noise.

We have reported in this paper the transition phenomena from torus to chaos of a symmetrically coupled logistic map. Numerical calculations were carried

out using mainly the double precision.

Acknowledgements

The author would like to thank Professor M. Suzuki for continual encouragement and critical reading of the manuscript. He would also like to thank Dr. I. Tsuda and Mr. S. Takesue for useful discussions. He wishes to thank Laboratory of International Collaboration on Elementary Particle Physics, for the fascilities of FACOM M190. This study was partially financed by the Scientific Reseach Fund of the Ministry of Education, Science and Culture.

References

1) D. Ruelle and F. Takens, Comm. Math. Phys. **20** (1971), 167.
2) J. P. Gollub and S. V. Benson, J. Fluid Mech. **100** (1980), 449.
3) S. Fauve and A. Libchaber, in *Chaos and Order in Nature*, ed. H. Haken (Springer, 1981).
4) D. G. Aronson, M. A. Chory, G. R. Hall and R. P. McGehee, Comm. Math. Phys. **83** (1982), 303.
5) S. J. Shenker, Physica **5D** (1982), 405.
6) M. J. Feigenbaum, L. P. Kadanoff and S. J. Shenker, Physica **5D** (1982), 370.
D. Rand, S. Ostlund, J. Sethna and E. D. Siggia, Phys. Rev. Letters **49** (1982), 132.
H. Daido, preprint.
7) L. Glass and R. Perez, Phys. Rev. Letters **48** (1982), 1772.
M. R. Guevara and L. Glass, J. Math. Biol. **14** (1982), 1.
8) K. Kaneko, Prog. Theor. Phys. **68** (1982), 669.
9) K. Kaneko, Prog. Theor. Phys. **69** (1983), 403.
10) H. Fujisaka and T. Yamada, preprint.
11) I. Schreiber and M. Marek, Phys. Letters **91A** (1982), 263.
12) M. Sano and Y. Sawada, private communication.
13) O. E. Rössler, Phys. Letters **71A** (1979), 155.
14) P. Collet and J. P. Eckmann, *Iterated Maps on the Intervals as Dynamical Systems* (Birkhäuser, 1980).
15) S. Takesue and K. Kaneko, to be published.
16) M. Suzuki, Adv. in Chem. Phys. **46** (1981) 195 and references cited therein.
17) I. Tsuda, Phys. Letters **85A** (1981), 4.
S. Aubry, in *Solitons and Condensed Matter Physics*, ed. A. R. Bishop and T. Schneider (Springer, 1978).
18) B. B. Mandelbrot, *Fractals-Form, Chance and Dimensions* (Freeman, San Francisco, 1977).
H. Mori, Prog. Theor. Phys. **63** (1980), 1044.
J. Kaplan and J. Yorke, in *Springer Lecture Notes in Mathematics* 730 (1979), 204.
19) J. P. Eckmann, Rev. Mod. Phys. **53** (1981), 643.
20) M. J. Feigenbaum, J. Stat. Phys. **19** (1978), 25.
21) Y. Pomeau and P. Manneville, Comm. Math. Phys. **74** (1980), 189.
22) K. Kaneko, to be published.
23) Heisenberg emphasized the importance of linearization, *symmetry*, unpredictability, and statistical methods for nonlinear problems; W. Heisenberg, Physics Today **20** (1967), 27.